JACS
JOURNAL OF THE AMERICAN CHEMICAL SOCIETY
Communication
pubs.acs.org/JACS

Total Structure and Optical Properties of a Phosphine/Thiolate-Protected Au_{24} Nanocluster

Anindita Das,[†] Tao Li,[‡] Katsuyuki Nobusada,[§] Qiong Zeng,[†] Nathaniel L. Rosi,[‡] and Rongchao Jin*[,†]

[†]Department of Chemistry, Carnegie Mellon University, Pittsburgh, Pennsylvania 15213, United States
[‡]Department of Chemistry, University of Pittsburgh, Pittsburgh, Pennsylvania 15260, United States
[§]Department of Theoretical and Computational Molecular Science, Institute for Molecular Science, Myodaiji, Okazaki, 444-8585, Japan

Supporting Information

ABSTRACT: We report the synthesis and total structure determination of a Au_{24} nanocluster protected by mixed ligands of phosphine and thiolate. Single crystal X-ray crystallography and electrospray ionization mass spectrometry (ESI-MS) unequivocally determined the cluster formula to be $[Au_{24}(PPh_3)_{10}(SC_2H_4Ph)_5X_2]^+$, where X = Cl and/or Br. The structure consists of two incomplete (i.e., one vertex missing) icosahedral Au_{12} units joined by five thiolate linkages. This structure shows interesting differences from the previously reported vertex-sharing biicosahedral $[Au_{25}(PPh_3)_{10}(SC_2H_4Ph)_5X_2]^{2+}$ nanocluster protected by the same type and number of phosphine and thiolate ligands. The optical absorption spectrum of Au_{24} nanocluster was theoretically reproduced and interpreted.

Revealing the atom packing structures of metal nanoclusters is of critical importance for understanding the quantum size effects in nanoclusters and evolution from molecular to plasmonic properties.[1] Over the past few years, a number of thiolate-protected gold nanoclusters with sizes larger than 10 gold atoms have been reported.[2−13] However, with respect to phosphine-protected gold nanoclusters, much fewer have been attained. Since the early report of $Au_{11}(PPh_3)_7(SCN)_3$ by McPartlin et al. in 1969,[14] Mingos et al. predicted the centered icosahedral Au_{13} cluster[15] and later successfully synthesized and determined this structure in 1981.[16] Diphosphine-protected Au_{13} icosahedral cluster has also been reported by Shichibu et al.[17a,b] and smaller ones have been synthesized by Pettibone et al.[17c] Teo and co-workers reported the structure of $[Au_{39}(PPh_3)_{14}Cl_6]Cl_2$.[18] A larger gold:phosphine cluster (formulated as $Au_{55}(PPh_3)_{12}Cl_6$) was reported by Schmid et al.,[19] which has since garnered much interest,[20] but its crystal structure has not been solved till date. Recently, Wan et al. reported the structure of a $[Au_{20}(PPhpy_2)_{10}Cl_4]^{2+}$ cluster that is composed of two edge-shared Au_{11} units and is protected by pyridyl phosphine ($Phpy_2$) ligands.[21] With phosphine/thiolate ligands, Shichibu et al.[22] attained a biicosahedral $[Au_{25}(PPh_3)_{10}(SC_2H_5)_5Cl_2]^{2+}$ cluster, which was synthesized from the phosphine-protected Au_{11} cluster (as precursor) through thiol etching.[23] This structure is related to the bimetal $[Au_{13}Ag_{12}(PR_3)_{10}X_7]^{2+}$ cluster (where X = halide) reported earlier by Teo et al.[24] We used a different thiol (HSC_2H_4Ph) to convert size-mixed 1−3.5 nm Au:phosphine nanoparticles (as opposed to Au_{11}:phosphine clusters[22]) into monodisperse $[Au_{25}(PPh_3)_{10}(SC_2H_4Ph)_5Cl_2]^{2+}$ clusters[25] and solved the crystal structure;[26] it exhibited the same structure as that of the $-SCH_2CH_3$ analogue.[22] Park and Lee[27] recently studied the electrochemical properties of the biicosahedral $[Au_{25}(PPh_3)_{10}(SR)_5Cl_2]^{2+}$ clusters with various thiolate ligands and found distinct differences from the electrochemical behavior of the all-thiolate protected $Au_{25}(SR)_{18}$ cluster.

In this work, we report a new $[Au_{24}(PPh_3)_{10}(SC_2H_4Ph)_5X_2]^+$ cluster (where X = Cl/Br) that is just one atom smaller than the previous $[Au_{25}(PPh_3)_{10}(SC_2H_4Ph)_5Cl_2]^{2+}$ cluster. This new cluster exhibits interesting differences in structural features and optical properties from those of the Au_{25} cluster.[22,26]

Details of the synthesis are provided in the Supporting Information. Briefly, we started with $HAuCl_4{\cdot}3H_2O$, rather than the commonly used $Au(PPh_3)Cl$ salt. $HAuCl_4{\cdot}3H_2O$ was first dissolved in water, then phase transferred to toluene with the aid of tetraoctylammonium bromide (TOAB). Then, PPh_3 was added to convert Au(III) to Au(I), followed by further reduction by $NaBH_4$. After 16 h, toluene was rotavaporated and the reddish brown product was extracted with dichloromethane. Phenylethylthiol was added to this solution and then reacted at 313 K for ∼4 h, after which excess PPh_3 was added and the reaction continued for an extra 24 h. Finally, $[Au_{24}(PPh_3)_{10}(SC_2H_4Ph)_5X_2]^+$ (counterion (X) = halide ions) was obtained. It is worth noting the difference in the synthesis of Au_{24} and Au_{25} nanoclusters. The first stage of the Au_{24} synthesis is similar to that of Au_{25}, but for obtaining Au_{24} nanoclusters, excess PPh_3 was added to the crude product from thiol etching at 313 K. The addition of excess PPh_3 in the last step is critical for obtaining Au_{24} nanoclusters.

Single crystals of Au_{24} nanoclusters were grown by vapor diffusion of hexane into a toluene solution of clusters. The crystal structure of $[Au_{24}(PPh_3)_{10}(SC_2H_4Ph)_5X_2]^+$ was found to have a triclinic space group $P\bar{1}$ (see Supporting Information). The rod-like core framework is shown in Figure 1. The cluster comprises a Au_{24} metal core (Figure 1, left), which may be viewed as two incomplete (i.e., one-vertex missing) icosahedral Au_{12} units joined together in an eclipsed fashion through five thiolate linkages (Figure 1, right). The diameter of the rod is 0.5 nm (Au atomic center-to-center distance) or 0.8 nm (edge-to-edge distance), and the length of the rod is 1.1 nm (Au center-to-

Received: October 14, 2012
Published: December 10, 2012

dx.doi.org/10.1021/ja3101566 | J. Am. Chem. Soc. 2012, 134, 20286−20289

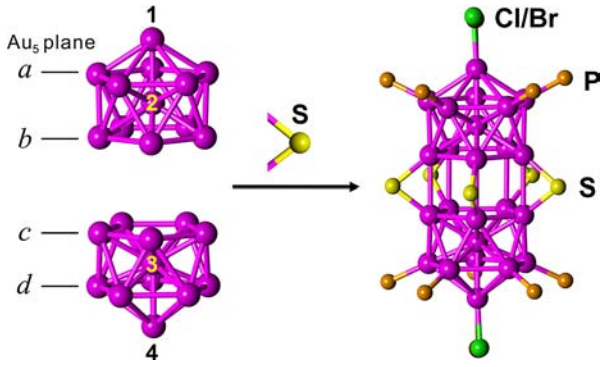

Figure 1. The core structure of $[Au_{24}(PPh_3)_{10}(SC_2H_4Ph)_5X_2]^+$. (color labels: magenta = Au; yellow = S; orange = P; green = Cl (partial occupancy) and brown = Br (partial occupancy).

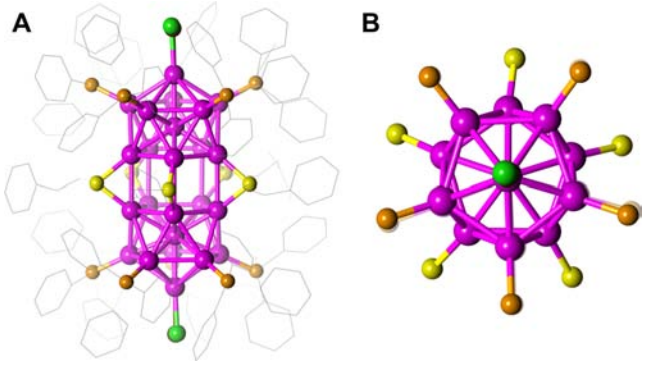

Figure 2. (A) Total structure of $[Au_{24}(PPh_3)_{10}(SC_2H_4Ph)_5X_2]^+$ cluster (color labels: gray = C, the rest are the same as specified in Figure 1.) (B) Top view of the $Au_{24}P_{10}S_5X_2$ core framework.

center) or 1.4 nm (edge-to-edge), where the diameter of Au atom is taken to be ~0.3 nm. The Au−S bond length is 2.375 ± 0.004 Å. The top and bottom Au_5 pentagons (Figure 1, atomic planes *a* and *d*) are coordinated to 10 PPh_3 ligands (Au−P bond length: 2.293 ± 0.007 Å). The two apex gold atoms (Figure 1 , labeled 1 and 4) are coordinated by halides (X = Br or Cl); both halide sites show partial occupancy of Cl and Br, resulting in three combinations, Br_2, Br/Cl, and Cl_2 (as observed in mass spectrometric analysis, vide infra), and the average Au−X bond length is 2.454 Å. There are two uncoordinated gold atoms, which are located in the centers of the two incomplete icosahedrons (Figure 1, labeled 2 and 3). Overall, the Au_{24} core adopts a quasi-D_{5h} symmetry. The total structure of $[Au_{24}(PPh_3)_{10}(SC_2H_4Ph)_5X_2]^+$ is shown in Figure 2A, and a top view of the $Au_{24}P_{10}S_5X_2$ framework is shown in Figure 2B, in which one can explicitly see the eclipsed structure.

Compared to the previously reported $[Au_{25}(PPh_3)_{10}(SR)_5Cl_2]^{2+}$ (R = C_2H_5 or C_2H_4Ph) cluster, which exhibits a *vertex-sharing* biicosahedral structure,[22,26] the most intriguing feature of $[Au_{24}(PPh_3)_{10}(SC_2H_4Ph)_5Cl_2]^+$ lies in that the central Au atom (i.e., the shared vertex atom in biicosahedral Au_{25}) is missing. The dislodgement of this central Au atom results in stronger interactions between the two Au_{12} incomplete icosahedrons in Au_{24}, manifested in the shorter Au_5−Au_5 interplane distance (Figure 1, planes *b* and *c*): 2.925 ± 0.011 Å in Au_{24} versus 3.053 ± 0.035 Å in Au_{25}. The 0.13 Å difference (−4.2% relative to Au_{25}) is quite significant. Moreover, the Au−Au distances within plane *b* and *c* are also shorter (−3.5% and −3%, respectively) than the corresponding values in Au_{25} (Table 1). The other Au−Au

Table 1. Comparison of $[Au_{24}(PPh_3)_{10}(SC_2H_4Ph)_5X_2]^+$ and $[Au_{25}(PPh_3)_{10}(SC_2H_4Ph)_5Cl_2]^{2+}$ Crystal Structures

Au−Au distances	Au_{24}, Å	Au_{25}, Å	dif.
$Au_{(1)}$ to pentagon *a*	2.990 ± 0.013	2.920 ± 0.030	+2.4%
within plane *a*	2.925 ± 0.010	2.929 ± 0.030	−0.1%
$Au_{(2)}$ to pentagon *a*	2.728 ± 0.011	2.755 ± 0.034	−1%
$Au_{(2)}$ to pentagon *b*	2.761 ± 0.008	2.801 ± 0.024	−1.4%
between *a* and *b*	2.923 ± 0.072	2.931 ± 0.021	−0.3%
within plane *b*	**2.802 ± 0.007**	**2.903 ± 0.022**	**−3.5%**
between *b* and *c*	**2.925 ± 0.011**	**3.053 ± 0.035**	**−4.2%**
within plane *c*	**2.802 ± 0.013**	**2.886 ± 0.012**	**−3%**
between *c* and *d*	2.922 ± 0.056	2.894 ± 0.030	+0.9%
$Au_{(3)}$ to pentagon *c*	2.756 ± 0.004	2.801 ± 0.026	−1.6%
$Au_{(3)}$ to pentagon *d*	2.721 ± 0.008	2.744 ± 0.022	−0.8%
within plane *d*	2.915 ± 0.011	2.953 ± 0.027	−1.3%
$Au_{(4)}$ to pentagon *d*	2.976 ± 0.026	2.983 ± 0.040	−0.2%

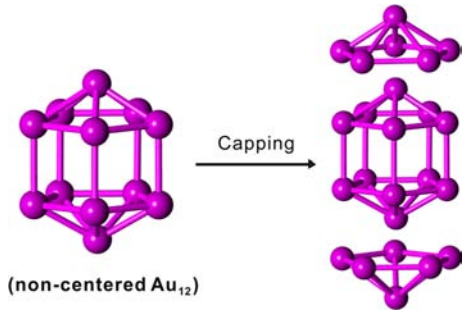

Figure 3. A different anatomy of the Au_{24} structure. (Left) An Au_{12} noncentered bicapped pentagonal prism; (right) capping by two roof-like Au_6 units.

distances in Au_{24} are less affected in comparison with Au_{25} (see Table 1). Overall, the observed shrinking at the "waist" of the cluster due to one-atom loss is quite distinct and may induce significant perturbation to the electronic structure and optical properties (vide infra).

The Au_{24} nanocluster structure is interesting in that it exhibits two Au_{12} incomplete icosahedrons with two pentagonal planes joined together by five thiolate linkages. This configuration does not involve any of the already observed structural modes such as vertex-sharing[24] via one gold atom in the $[Au_{25}(PPh_3)_{10}(SR)_5X_2]^{2+}$ rod,[22,26] edge-sharing via two atoms in the $[Au_{20}(PPhpy_2)_{10}Cl_4]^{2+}$ rod,[21] or face-sharing via three atoms in the $Au_{38}(SC_2H_4Ph)_{24}$ rod.[8] The Au_{24} core structure observed in this work is different from the "cluster of clusters" model discussed earlier by Teo et al.,[24] according to which sequential accretion of 13-atom icosahedral building blocks leads to larger clusters via vertex sharing. One may argue that the clusters reported by Teo et al. involved phosphine and halide ligands but without thiolate; halide (X = Cl, Br) would be different from thiolate in terms of ligation. However, recent theoretical studies by Jiang et al. implied that halides as ligands behave in much the same way as thiolate.[28] Therefore, introducing thiolate ligands should not be the cause of the new structure of Au_{24} and its production as opposed to Au_{25}. Detailed studies on the growth mechanism are underway.

Another view of the Au_{24} structure is a *non*-centered, bicapped pentagonal prismatic Au_{12} core (Figure 3, left) further capped by two pentagonal "hats" (Figure 3, right). To the best of our knowledge, this *non*-centered pentagonal prismatic structural motif is unprecedented in gold cluster structures.

dx.doi.org/10.1021/ja3101566 | J. Am. Chem. Soc. 2012, 134, 20286−20289

To confirm the cluster formula and probe the charge state of the cluster, we further performed electrospray ionization mass spectrometric analysis (ESI-MS). Positive ion mode ESI-MS (Figure 4) revealed a set of prominent peaks of intact cluster ions

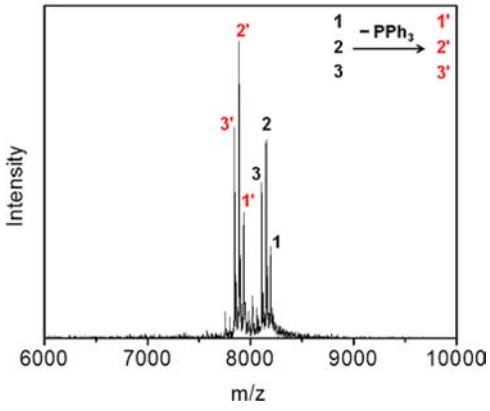

Figure 4. ESI-MS spectrum of $[Au_{24}(PPh_3)_{10}(SC_2H_4Ph)_5X_2]^+$ (positive mode). 1−3 corresponding to intact cluster ions (z = +1) with X = Br, Br/Cl (0.5/0.5), and Cl, respectively; 1′−3′ corresponding to one-PPh_3-lost cluster ions (z = +1) with X = Br, Br/Cl (0.5/0.5), and Cl, respectively.

1−**3** at m/z = 8196.63 (peak **1**, $[Au_{24}(PPh_3)_{10}(SC_2H_4Ph)_5\mathbf{Br_2}]^+$), 8151.76 (peak **2**, $[Au_{24}(PPh_3)_{10}(SC_2H_4Ph)_5\mathbf{BrCl}]^+$) and 8107.42 (peak **3**, $[Au_{24}(PPh_3)_{10}(SC_2H_4Ph)_5\mathbf{Cl_2}]^+$). Of note, fragmentation (i.e., loss of *one phosphine*) occurred quite severely in ESI process, with one PPh_3 missing cluster peaks **1′**−**3′** observed at m/z = 7934.57 (peak **1′**, $[Au_{24}(PPh_3)_9(SC_2H_4Ph)_5Br_2]^+$), 7889.41 (peak **2′**, $[Au_{24}(PPh_3)_9(SC_2H_4Ph)_5BrCl]^+$) and 7844.71 (peak **3′**, $[Au_{24}(PPh_3)_9(SC_2H_4Ph)_5Cl_2]^+$), respectively. The loss of phosphine in ESI-MS was also observed in $[Au_{20}(PPhpy_2)_{10}Cl_4]^{2+}$ as reported recently.[21]

The difference between Au_{24} and Au_{25} nanoclusters also lies in the optical properties. The UV−vis spectrum of $[Au_{24}(PPh_3)_{10}(SC_2H_4Ph)_5X_2]^+$ in dichloromethane (Figure 5a) shows prominent bands at 383 and 560 nm (broad). In contrast, $[Au_{25}(PPh_3)_{10}(SC_2H_4Ph)_5Cl_2]^{2+}$ nanoclusters[25,26] show absorption bands at 415 and 670 nm (Figure 5b, similar to the SC_2H_5 counterpart[22]). Previously, density functional theory (DFT) calculations on the Au_{25} nanocluster by Nobusada et al.[29] revealed that the 670 nm band is the HOMO−LUMO transition in the Au_{25} cluster and is caused by the interactions between the two complete icosahedral Au_{13} units. The observed differences in optical spectra between Au_{24} and Au_{25} nanoclusters indicate the distinct effects of a single gold atom on the cluster's electronic structure and optical properties. It is also worth noting that, unlike the phosphine- and thiolate-protected Au_{20} clusters which exhibit similar optical spectra (Figure S1),[21,30] $[Au_{24}(PPh_3)_{10}(SC_2H_4Ph)_5X_2]^+$ and $Au_{24}(SC_2H_4Ph)_{20}$ clusters[31] indeed exhibit quite different spectra (Figure S2). Further insight into their optical properties has to wait until the attainment of the crystal structures of $Au_{20}(SR)_{16}$ and $Au_{24}(SR)_{20}$.

To interpret the optical spectrum of the $[Au_{24}(PPh_3)_{10}(SC_2H_4Ph)_5X_2]^+$ nanocluster, we have carried out DFT calculations[32] of a model cluster mimicking the present Au_{24} nanocluster (see details of the calculations in the Supporting Information). The DFT results are in good agreement with the experimental observations of the geometric structure and optical absorption spectrum. The optimized geometric structure of the Au_{24} core cluster slightly expands (<∼ 2.5%) in comparison with the determined crystal structure, while the Au_{12} − Au_{12} distance is more prolonged (∼ 5.5%) than the experimental structure.

The computed absorption spectrum, which is convoluted by the Lorentz function with appropriate width, is shown in Figure 5c. The peak positions and spectral pattern are reasonably reproduced by DFT calculations. The simulated, lowest-energy peak is at 510 nm (Figure 5c), which corresponds to the experimentally observed broad band at ∼560 nm; the ∼0.2 eV discrepancy is in large part due to the limitation of accuracy of DFT calculations.[33] This absorption peak arises from the HOMO−1 to LUMO+2 electronic transition. The LUMO+2 is a localized molecular orbital and mainly distributed around the Au_{12}−Au_{12} junction (Figure 5d). Thus, this electronic transition

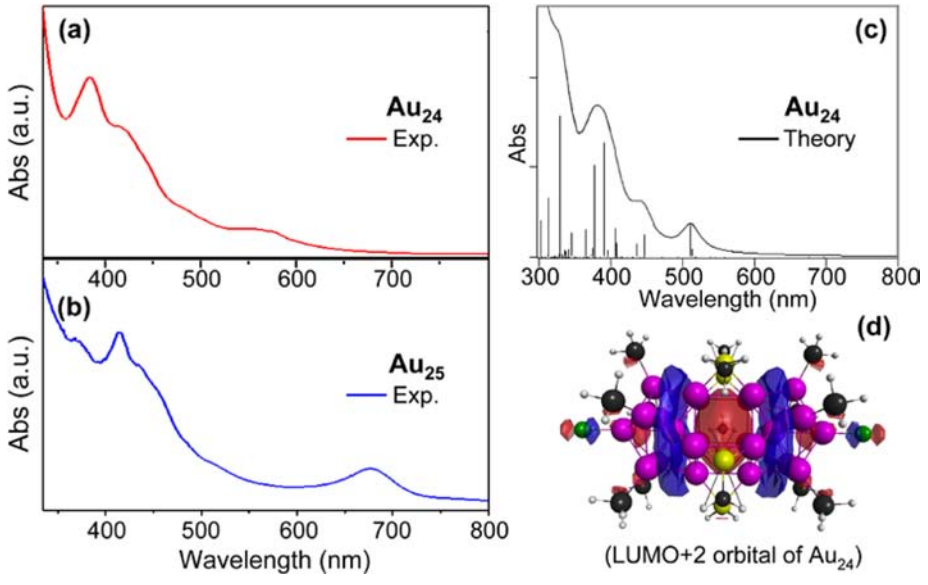

Figure 5. (a) Experimental optical spectrum of $[Au_{24}(PPh_3)_{10}(SC_2H_4Ph)_5X_2]^+$ (in dichloromethane), (b) experimental optical spectrum of $[Au_{25}(PPh_3)_{10}(SC_2H_4Ph)_5X_2]^{2+}$ (in dichloromethane), (c) DFT simulated optical spectrum of $[Au_{24}(PH_3)_{10}(SCH_3)_5X_2]^+$ model cluster, and (d) the LUMO+2 molecular orbital of $[Au_{24}(PH_3)_{10}(SCH_3)_5X_2]^+$.

dx.doi.org/10.1021/ja3101566 | J. Am. Chem. Soc. 2012, 134, 20286−20289

has a character similar to the Au_{25} cluster's HOMO to LUMO transition[29] (Figure 5b, the lowest-energy peak at ~670 nm) in the sense that both are caused by interactions between the two units (i.e., Au_{12}–Au_{12} in the Au_{24} cluster and Au_{13}–Au_{13} in the Au_{25} cluster).

For other optical features of Au_{24}, the calculated peak at ~440 nm (Figure 5c) is well assigned to the experimental 415 nm shoulder (Figure 5a), and the simulated ~380 nm peak to the experimental 383 nm band; both spectral features are primarily due to the electronic transitions related to the localized electronic structures of the individual Au_{12} unit.

With respect to the photoluminescence (PL) properties of the phosphine/thiolate-capped Au_{24} cluster, it exhibits a weak PL band centered at ~818 nm and the excitation spectrum for this PL band resembles the absorption spectrum (Figure S3). The 818 nm emission of Au_{24} is comparable to that of Au_{25} cluster[27] and may involve surface states.

We also performed cyclic voltammetry (CV) measurements to probe the HOMO–LUMO gap (Figure S4). The electrochemical gap between the oxidation onset (+0.3 V vs Ag/Ag^+) and reduction onset (−1.05 V vs Ag/Ag^+) is ~1.35 eV, which is slightly smaller than that of Au_{25} (E_g~1.54 eV).[27]

Finally, it should be pointed out that gold clusters protected by the binary phosphine/thiolate ligands are significantly more stable than those protected by phosphine only. The latter tends to photodegrade slowly, but for PPh_3/thiolate-protected Au_{24} (e.g., crystals or powders), we did not observe degradation of the clusters under ambient conditions after several months (longer time not tested).

In summary, this work reports the synthesis and crystal structure determination of a new $[Au_{24}(PPh_3)_{10}(SC_2H_4Ph)_5X_2]^+$ (counterion: X = halide) nanocluster protected by phosphine/thiolate ligands. This Au_{24} nanocluster exhibits distinct differences from the previously reported Au_{25} nanocluster in the structure and optical properties. DFT calculations reproduced the optical absorption spectrum and interpreted the optical features, which can be divided into high-energy electronic transitions within individual Au_{12} units and a low-energy unique transition due to interactions between two Au_{12} units. The mechanism of preferential growth of $[Au_{24}(PPh_3)_{10}(SC_2H_4Ph)_5X_2]^+$ over $[Au_{25}(PPh_3)_{10}(SC_2H_4Ph)_5X_2]^{2+}$ remains to be unraveled in future work.

■ ASSOCIATED CONTENT

Supporting Information

Details of the synthesis, X-ray crystallographic analysis, DFT calculations, and supporting Figures S1–S4. This material is available free of charge via the Internet at http://pubs.acs.org.

■ AUTHOR INFORMATION

Corresponding Author

rongchao@andrew.cmu.edu

Notes

The authors declare no competing financial interest.

■ ACKNOWLEDGMENTS

R.J. thanks the support by the Air Force Office of Scientific Research under AFOSR Award No. FA9550-11-1-9999 (FA9550-11-1-0147) and the Camille Dreyfus Teacher-Scholar Awards Program. K.N. acknowledges research support by Grant-in-Aid (No. 21350018) and by Next Generation Supercomputer Project from the Ministry of Education, Culture, Sports, Science and Technology (MEXT) of Japan. We thank Dr. Zhongrui Zhou for assistance in ESI-MS analysis and the University of Pittsburgh for permitting us to access the X-ray diffractometer.

■ REFERENCES

(1) Qian, H.; Zhu, M.; Wu, Z.; Jin, R. *Acc. Chem. Res.* **2012**, *45*, 1470.
(2) Nishigaki, J.; Tsunoyama, R.; Tsunoyama, H.; Ichikuni, N.; Yamazoe, S.; Negishi, Y.; Ito, M.; Matsuo, T.; Tamao, K.; Tsukuda, T. *J. Am. Chem. Soc.* **2012**, *134*, 14295.
(3) Zhu, M.; Aikens, C. M.; Hollander, F. J.; Schatz, G. C.; Jin, R. *J. Am. Chem. Soc.* **2008**, *130*, 5883.
(4) Dass, A.; Stevenson, A.; Dubay, G. R.; Tracy, J. B.; Murray, R. W. *J. Am. Chem. Soc.* **2008**, *130*, 5940.
(5) (a) Yu, Y.; Luo, Z.; Yu, Y.; Lee, J. Y.; Xie, J. *ACS Nano* **2012**, *6*, 7920. (b) Krommenhoek, P. J.; Wang, J.; Hentz, N.; Johnston-Peck, A. C.; Kozek, K. A.; Kalyuzhny, G.; Tracy, J. B. *ACS Nano* **2012**, *6*, 4903.
(6) (a) Aikens, C. M. *J. Phys. Chem. Lett.* **2011**, *2*, 99. (b) Jung, J.; Kang, S.; Han, Y.-K. *Nanoscale* **2012**, *4*, 4206.
(7) Nimmala, P. R.; Dass, A. *J. Am. Chem. Soc.* **2011**, *133*, 9175.
(8) Qian, H.; Eckenhoff, W. T.; Zhu, Y.; Pintauer, T.; Jin, R. *J. Am. Chem. Soc.* **2010**, *132*, 8280.
(9) Muhammed, M. A. H.; Verma, P. K.; Pal, S. K.; Kumar, R. C. A.; Paul, S.; Omkumar, R. V.; Pradeep, T. *Chem.–Eur. J.* **2009**, *15*, 10110.
(10) (a) Levi-Kalisman, Y.; Jadzinsky, P. D.; Kalisman, N.; Tsunoyama, H.; Tsukuda, T.; Bushnell, D. A.; Kornberg, R. D. *J. Am. Chem. Soc.* **2011**, *133*, 2976. (b) Grönbeck, H. *Nanoscale* **2012**, *4*, 4178.
(11) Heinecke, C. L.; Ni, T. W.; Malola, S.; Mäkinen, V.; Wong, O. A.; Häkkinen, H.; Ackerson, C. J. *J. Am. Chem. Soc.* **2012**, *134*, 13316.
(12) (a) Qian, H.; Jin, R. *Nano Lett.* **2009**, *9*, 4083. (b) Qian, H.; Zhu, Y.; Jin, R. *Proc. Natl. Acad. Sci. U.S.A.* **2012**, *109*, 696.
(13) (a) Negishi, Y.; Kurashige, W.; Niihori, Y.; Iwasa, T.; Nobusada, K. *Phys. Chem. Chem. Phys.* **2010**, *12*, 6219. (b) Kumara, C.; Dass, A. *Nanoscale* **2011**, *3*, 3064. (c) Qian, H.; Jiang, D.-e.; Li, G.; Gayathri, C.; Das, A.; Gil, R. R.; Jin, R. *J. Am. Chem. Soc.* **2012**, *134*, 16159.
(14) McPartlin, M.; Mason, R.; Malatesta, L. *J. Chem. Soc. D* **1969**, 334.
(15) Mingos, D. M. P. *J. Chem. Soc., Dalton Trans.* **1976**, 1163.
(16) Briant, C. E.; Theobald, B. R. C.; White, J. W.; Bell, L. K.; Mingos, D. M. P.; Welch, A. J. *J. Chem. Soc., Chem. Commun.* **1981**, 201.
(17) (a) Shichibu, Y.; Konishi, K. *Small* **2010**, *6*, 1216. (b) Shichibu, Y.; Suzuki, K.; Konishi, K. *Nanoscale* **2012**, *4*, 4125. (c) Pettibone, J. M.; Hudgens, J. W. *J. Phys. Chem. Lett.* **2010**, *1*, 2536.
(18) Teo, B. K.; Shi, X.; Zhang, H. *J. Am. Chem. Soc.* **1992**, *114*, 2743.
(19) Schmid, G.; Pfeil, R.; Boese, R.; Bandermann, F.; Meyer, S.; Calis, G. H. M.; van der Velden, J. W. A. *Chem. Ber.* **1981**, *114*, 3634.
(20) (a) Schmid, G. *Chem. Soc. Rev.* **2008**, *37*, 1909. (b) Torma, V.; Schmid, G.; Simon, U. *Chem. Phys. Chem.* **2001**, *5*, 321.
(21) Wan, X.-K.; Lin, Z.-W.; Wang, Q.-M. *J. Am. Chem. Soc.* **2012**, *134*, 14750.
(22) Shichibu, Y.; Negishi, Y.; Watanabe, T.; Chaki, N. K.; Kawaguchi, H.; Tsukuda, T. *J. Phys. Chem. C* **2007**, *111*, 7845.
(23) Woehrle, G. H.; Warner, M. G.; Hutchison, J. E. *J. Phys. Chem. B* **2002**, *106*, 9979.
(24) (a) Teo, B. K.; Zhang, H. *Inorg. Chem.* **1991**, *30*, 3115. (b) Teo, B. K.; Zhang, H. *Coord. Chem. Rev.* **1995**, *143*, 611.
(25) Qian, H.; Zhu, M.; Lanni, E.; Zhu, Y.; Bier, M. E.; Jin, R. *J. Phys. Chem. C* **2009**, *113*, 17599.
(26) Qian, H.; Eckenhoff, W. T.; Bier, M. E.; Pintauer, T.; Jin, R. *Inorg. Chem.* **2011**, *50*, 10735.
(27) Park, S. Y.; Lee, D. *Langmuir* **2012**, *28*, 7049.
(28) Jiang, D.-e.; Walter, M. *Nanoscale* **2012**, *4*, 4234.
(29) Nobusada, K.; Iwasa, T. *J. Phys. Chem. C* **2007**, *111*, 14279.
(30) Zhu, M.; Qian, H.; Jin, R. *J. Am. Chem. Soc.* **2009**, *131*, 7220.
(31) Zhu, M.; Qian, H.; Jin, R. *J. Phys. Chem. Lett.* **2010**, *1*, 1003.
(32) (a) Nobusada, K. *J. Phys. Chem. B* **2004**, *108*, 11904. (b) Iwasa, T.; Nobusada, K. *J. Phys. Chem. C* **2007**, *111*, 45.
(33) Reimers, J. R.; Wang, Y.; Cankurtaran, B. O.; Ford, M. J. *J. Am. Chem. Soc.* **2010**, *132*, 8378.